RESEARCH PAPER

Deep Learning–Based Multi-Class Brain Tumor Classification Using an Enhanced CNN Architecture

Mohammed Razia Alangir Banu[1*], Sumit Hazra[2], A S Gousia Banu[1]

[1]Research Scholar, Department of Computer Science and Engineering, Koneru Lakshmiah Education Foundation, Hyderabad, India.

[2]Assistant Professor & AI&ML Research Group Head, Department of Computer Science and Engineering, Koneru Lakshmiah Education Foundation, Hyderabad, India.

ABSTRACT

Brain tumours (BTs) are increasing rapidly worldwide and remain a leading cause of death for thousands of individuals each year. Recent advances in computer vision and image processing have significantly improved diagnostic accuracy while reducing costs and processing time, ultimately transforming healthcare technology. Radiologists commonly turn to magnetic resonance imaging (MRI) due to its exceptional sensitivity in detecting even the smallest anomalies within the brain. Over the years, researchers have introduced numerous methods for identifying and classifying brain tumours. Most of these approaches fall into two categories: traditional machine learning (ML) or deep learning (DL). Classical ML classifiers, however, come with a notable drawback—they require manually crafted features, making the process labour-intensive and time-consuming. Deep learning has emerged as a powerful alternative, gaining widespread adoption for both detection and classification tasks. Its primary strength lies in automatic feature extraction, eliminating the need for manual intervention. Building on this foundation, we present DeepTumorNet, a hybrid deep learning model that classifies three distinct types of brain tumours—gliomas, meningiomas, and pituitary tumours—using a convolutional neural network (CNN) architecture. Our journey began with GoogLeNet, a well-established CNN framework. To tailor it specifically for brain tumour classification, we converted it into a hybrid model by removing the final five layers and adding fifteen additional layers. This modification deepened the network and enhanced its learning capacity. Furthermore, we incorporated a leaky ReLU activation function within the feature maps, which improved the model's expressiveness and allowed it to capture more nuanced patterns. To evaluate its effectiveness, we conducted extensive experiments using a contrast-enhanced MRI (CE-MRI) dataset. The results were compelling: DeepTumorNet achieved an accuracy of 96.45%, precision of 95.32%, recall of 96.01%, and an F1 score of 95.20%. These figures consistently outperformed other contemporary approaches applied to the same dataset, underscoring the potential of our hybrid model as a reliable tool for assisting clinicians in accurate brain tumour diagnosis [31].

Keywords: Brain tumor classification, Deep learning, GoogLeNet, MRI images, Health care, Hyperparameters.

How to cite this article: Banu M R A, Hazra S, Banu A S G, Deep Learning–Based Multi-Class Brain Tumor Classification Using an Enhanced CNN Architecture. Int J Drug Deliv Technol. 2026;16(9s): 734-748; Doi: 10.25258/Ijddt.16.9s.77.

Source of support: Nil

Conflict of interest: None

INTRODUCTION

The human brain is one of the most complex organs in the body, containing about 100 billion nerve cells that control the entire nervous system [1]. Because it acts as the command center for almost all bodily functions, any problem in the brain can lead to serious health issues. One of the most serious problems is the development of tumors, which happen when cells start to grow abnormally and uncontrollably. Brain tumors are usually divided into two main groups: primary and secondary. Primary tumors start in the brain, while secondary tumors, also called metastatic tumors, begin in another part of the body and reach the brain through the bloodstream [2]. Some primary tumors are more common and dangerous than others. For example, glioma and meningioma are known to be aggressive and can be life-threatening if not found early [3]. Glioma is actually one of the most common types of primary brain tumors [4]. To help understand how serious these tumors are, the World Health Organization has created a system that sorts brain tumors into four grades [5]. Grades 1 and 2 are considered less severe and include tumors like meningioma. Grades 3 and 4 are more aggressive and include tumors like glioma. In practice, gliomas make up about 45% of cases, while meningiomas and pituitary tumors each account for around 15%. This breakdown

shows why it is important to classify tumors correctly, since treatment depends on the type, size, and exact location of the tumor. Right now, surgery is the main treatment for brain tumors, especially since modern methods try to reduce side effects on the nervous system [6]. But before surgery, doctors need to find and identify the tumor accurately. This is where medical imaging is essential. There are several ways to image the brain, such as computed tomography (CT), positron emission tomography (PET), and magnetic resonance imaging (MRI). Of these, MRI is the preferred method because it provides detailed two-dimensional and three-dimensional images of the tumor's type, size, shape, and location [6]. However, looking at MRI scans by hand can be difficult. It takes a lot of time and can lead to mistakes, especially as more patients need to be checked [7]. Because of these challenges, there is a strong need for automated solutions. A fully automated computer-aided diagnosis (CAD) system could help doctors and radiologists by reducing their workload and making diagnoses more consistent and accurate. To address this, researchers have worked on developing reliable ways to automatically classify brain tumors. Figure 1 shows the three main tumor types discussed in this study: glioma, meningioma, and pituitary tumors. This provides a visual reference for the classification task [32].

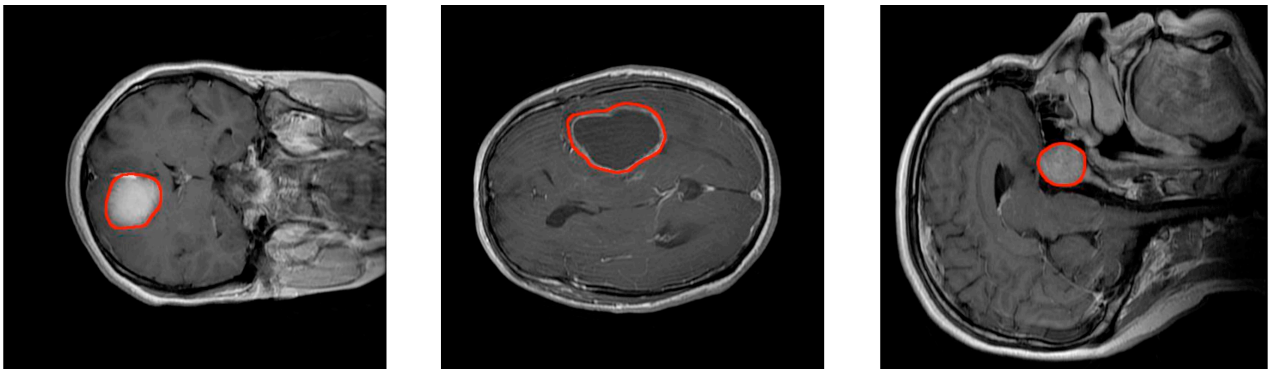

Figure 1. T1-CE MRI image dataset. Left: coronal view of a meningioma tumor. Centre: Axial view of a glioma tumor. Right: sagittal view of a pituitary tumor. Tumor borders have been highlighted in red.

In recent years, deep learning has emerged as a transformative technology, capturing the attention of researchers and practitioners across virtually every field—including medical image analysis [8]. What makes deep learning particularly powerful is its multi-layered architecture, which enables it to process vast amounts of unstructured data efficiently. Each layer gradually extracts features and passes them forward to the next, resulting in increasingly sophisticated representations and greater model flexibility [9]. At its core, deep learning excels at automatic feature extraction, eliminating the need for manual intervention and allowing models to uncover complex patterns directly from raw data. Among the various deep learning architectures, convolutional neural networks (CNNs) have become the dominant choice for medical image processing tasks. Their efficient processing capabilities make them ideally suited for extracting meaningful features and representations from the structured data found within medical images [10]. Recognizing this potential, we developed a deep learning–based approach aimed at improving both the performance and accuracy of existing algorithms for brain tumor classification. To validate our method, we tested it using a publicly available dataset. Our proposed solution, DeepTumorNet, is a hybrid deep learning model designed to detect and classify brain tumors into three primary types: meningiomas, pituitary tumors, and gliomas. The model leverages deep learning for robust feature extraction and incorporates a Softmax classification layer to handle multi-class differentiation effectively. When evaluated on the publicly available CE-MRI dataset, DeepTumorNet achieved the highest classification accuracy to date, outperforming traditional deep learning architectures such as AlexNet, ResNet50, SqueezeNet, DenseNet, DarkNet53, MobileNetV2, ResNet101, and ShuffleNet [11, 33].

The key contributions of our work can be summarised as follows:

- First, we introduce DeepTumorNet—a novel hybrid deep learning model specifically architected for the automatic classification of brain tumors into gliomas, meningiomas, and pituitary tumors using contrast-enhanced MRI (CE-MRI) scans. The model combines deep feature extraction with Softmax-based classification to deliver accurate and reliable results [34-40].
- Second, we conduct a rigorous evaluation of our proposed model on a publicly available CE-MRI dataset. The experimental results demonstrate that DeepTumorNet achieves superior classification accuracy compared to several state-of-the-art deep learning models, including AlexNet, ResNet50, SqueezeNet, DenseNet, DarkNet53, MobileNetV2, ResNet101, and ShuffleNet [41-50].

- Finally, our work advances the field of computer-aided diagnosis (CAD) by offering a highly accurate and fully automated solution. This has the potential to significantly reduce radiologists' workload, minimise manual diagnostic errors, and enable faster, more reliable detection of brain tumours in routine clinical practice [51].

The remainder of this paper is structured as follows. Section 2 reviews related work in the field. Section 3 provides a detailed explanation of our proposed methodology. Section 4 presents and discusses the experimental results. Finally, Section 5 concludes the study with a summary of findings and directions for future research.

LITERATURE SURVEY

This section presents a comprehensive review of contemporary deep learning approaches developed for brain tumor classification. Researchers have explored numerous strategies over the years, employing both deep learning and transfer learning techniques to address this challenging medical imaging task. Broadly speaking, modern methods can be grouped into three categories: deep learning–based approaches, machine learning–based techniques, and hybrid models that combine elements from both paradigms. Table 1 provides a summary of representative brain tumor classification methods discussed in the literature [52, 53].

In an innovative study, [12] proposed integrating a genetic algorithm with a convolutional neural network (CNN) for analyzing MR images. Notably, their approach did not rely on conventional trial-and-error experimentation; instead, the genetic algorithm guided the architecture design process. Through this method, they achieved accuracy values ranging up to an impressive 94.2%. The novelty of their work lies in successfully merging evolutionary computation with deep learning structures to optimize model performance [54].

Taking a different optimization-focused path, [13] introduced a fuzzy brainstorming technique for MR image classification. Their methodology unfolded across four key stages: image acquisition, enhancement, feature extraction, and final classification. Segmentation also formed an integral part of their pipeline. By fine-tuning optimization parameters alongside classification settings, they attained an accuracy of 93.85%, demonstrating how careful parameter adjustment can boost model effectiveness.

Meanwhile, [14] tackled the problem of classifying brain MRI scans into three distinct categories. Their approach began with preprocessing steps to prepare the images, followed by feature extraction using deep learning models. For the actual classification task, they turned to machine learning—specifically, the AdaBoost algorithm. Their efforts yielded an overall accuracy of 93.3%. However, it is worth noting that employing deep architectures for feature extraction can increase computational costs, particularly when dealing with large datasets [34, 55, 56].

In a separate investigation, [15] evaluated three well-known CNN architectures—AlexNet, ResNet50, and GoogleNet—using a dataset containing two classes of MRI images. Among these, ResNet50 delivered the highest performance, achieving an accuracy of 85.71%. While the study contributed valuable insights into tumour detection, its two-class dataset limited its ability to address the more nuanced challenge of identifying specific tumour stages [57, 58].

To overcome data scarcity issues, [16] proposed a novel CNN approach that first segmented tumor regions before classification. They tested their model on both original and multiplexed datasets, reporting an accuracy of 87.38% on the original data. This strategy of dataset augmentation helped mitigate the limitations imposed by the limited training samples [59, 60].

Expanding on architectural innovation, [17] developed a fully automated deep multi-scale 3D-CNN for brain image classification. Their workflow incorporated data enlargement and preprocessing techniques to enhance model robustness. Without preprocessing, their model achieved an accuracy of 87.7%, highlighting the importance of data preparation in achieving reliable results.

Recognizing that traditional CNN architectures often require substantial training data, [18] turned to capsule networks as an alternative. Their proposed method achieved an accuracy of 86.56%, compared to 82.30% obtained using the original dataset. These results suggest that capsule networks may offer advantages when working with sparse datasets, making them a promising direction for future research.

Another contribution came from [19], who developed a CNN-based model for brain tumor categorization without relying on segmentation. They created seven distinct CNN variants and evaluated them on the BraTS 2020 brain MRI dataset. Among these, their second variant achieved a training accuracy of 98.51% and a testing accuracy of 84.19%, outperforming earlier models in the study [61].

A more recent deep neural network–based multi-class model was introduced by [20]. Their system employed data augmentation techniques and leveraged a generative adversarial network (GAN) to learn structural patterns from BraTS 2019 images. By replacing the network's fully connected layers with a classifier, they

enabled accurate tumour type differentiation. Tested with five-fold cross-validation, the model achieved a 95.6% success rate with random splits and 93.01% with inserted splits, demonstrating strong generalisation capabilities.

Revisiting the genetic algorithm approach, [21] explored how evolutionary optimization could enhance CNN accuracy for brain tumor classification. By modifying the CNN architecture using a genetic algorithm, they achieved a peak accuracy of 94.2% on the Figshare dataset, reinforcing the potential of combining evolutionary strategies with deep learning [62].

In a similar vein, [22] proposed a multi-layer deep CNN designed to improve tumour classification accuracy [23]. Their model was evaluated across three datasets: BraTS 2018, Radiopaedia, and the Repository of Molecular Brain Neoplasia Data (REMBRANDT). Remarkably, it delivered strong performance with considerably less preprocessing than required by earlier methods, underscoring the efficiency gains possible through thoughtful architecture design.

Finally, [24] applied transfer learning techniques to enhance three-class brain tumour classification [25, 26]. Their model achieved an accuracy of 97.1% on MRI images obtained from Figshare, surpassing other systems trained on smaller datasets. Additionally, the researchers analysed instances of misclassification, offering valuable insights into the model's limitations and areas for improvement [63-66].

Table 1. Key studies on brain tumor classification using deep learning

Reference	Method	Dataset	Key Findings	Limitations
Nahiduzzaman et al. [2]	CNN-based Deep Learning Model	BraTS 2020	Achieved 92.5% accuracy in classifying glioma, meningioma, and pituitary tumors	Limited generalization due to small dataset size
Rao, C.S et al. [27]	Transfer Learning with ResNet-50	BraTS 2019 & Private MRI dataset	Improved classification accuracy (93.2%) with transfer learning	Requires high computational resources
Saleem et al. [28]	Hybrid CNN-RNN Model	BraTS 2018	Effective feature extraction from MRI sequences, achieving 91.8% accuracy	Performance drops in noisy MRI scans
PR. Kumar et al. [30]	3D U-Net + Deep Feature Extraction	Private Clinical MRI Dataset	Outperforms traditional CNN models with 95% classification accuracy	Not tested on publicly available datasets
Mostafa et al. [5]	VGG16 + SVM Classifier	Figshare Brain MRI Dataset	Achieved 90.5% accuracy in distinguishing tumor types	Overfitting issue in a small dataset scenario
Zhang et al. [9]	Deep CNN with Data Augmentation	BraTS 2017	Improved robustness to variations in MRI contrast and intensity	Requires extensive preprocessing and tuning

The study methodology and models that were described above have shortcomings, as can be seen from the analysis that was conducted above. In light of these constraints, this study suggests novel approaches to enhancing object (tumour) classification, dealing with low-quality features, improving classification performance on a small dataset, and increasing visibility in MRI images.

METHODOLOGY

In this part, the suggested study approach for fine-grained Brain Tumour (BTs) categorisation is outlined and discussed in detail. There are two basic phases to describe the proposed method. The research dataset used for fine-grained BTs categorisation was first described in detail. Secondly, we provided a detailed explanation of the architecture and proposed method for using deep learning to identify and categorise brain MRI scans as either meningiomas, gliomas, or pituitary tumours [67].

3.1 Dataset Description

Clinical settings sometimes only allow for a limited number of slices of brain CE-MRI, typically with a substantial slice gap, rather than acquiring and making available a 3D volume. Using such limited data to construct a 3D model is challenging. Therefore, the 2D slices obtained from 233 patients from a publicly available database form the basis of the proposed technique [5]. Gliomas (1,426 slices), pituitary tumors (930 slices), and meningiomas (708 slices) make up the 3,064 slices that make up this dataset. Also included in this dataset are 5-fold cross-validation indices. Using

this data, we train using 80% for training (2452 images) and 10% for testing (612 images). Furthermore, 10% of the training set (approximately 612 images). This procedure is carried out 50 times. The image's pixel size is 0.49 × 0.49 mm², and its in-plane resolution is 512 × 512 pixels. A 1 mm space between the slices, and each slice is 6 mm thick. Three seasoned radiologists carefully traced the tumor's edge by hand. A patient ID, the tumor type label (l_gt) (where 1 indicates meningioma, 2 gliomas, and 3 pituitary tumors), the x- and y-coordinates of the points on the tumor's border, and the tumor mask (T_ij)—a binary image with 1 for tumor positions and 0 for healthy ones—are all attached to each slice in the dataset. To begin training, the pair will serve as the baseline. To keep the neural network from becoming overfit during training, data augmentation with an elastic transform [3] has been employed. In Table 2, we can see the specifics of the study dataset [68].

Table 2. Explanation of the CE-MRI dataset

Tumor Class	Patients	Total Images	MRI view	Total MRI Images
Meningioma	81	709	A*	208
			C*	269
			S*	230
Pituitary	61	931	A*	292
			C*	318
			S*	321
Glioma	88	1427	A*	493
			C*	438
			S*	495
Sum	230	3067		3064

The class-specific data augmentation approach increased the amount of training images to 4,904 images, thus increasing their availability on each fold iteration. Each image in the training dataset had 65 × 65 training examples extracted using a meticulous approach. Each tumor had 325 true negative window samples and 150 true positive examples. Pixel standardization, which ensures that all pixels in a dataset have the same size and distribution across all training sets, was used to scale the pixels on these windows.

3.2 Feature Extraction

A pre-trained GoogleNet forms the basis of the feature extraction algorithm. As a feature extraction layer is pre-specified, the input image is allowed to propagate forward by the GoogleNet system, which functions as an arbitrary feature extractor. Here it stops, and we take the features that the layer produced as our basis. The suggested approach employs a pre-trained CNN deep learning model called Google-Net. Initialization layers in the Google-Net model incorporate different kernel sizes to give varying receptive fields. [7, 69, 70].

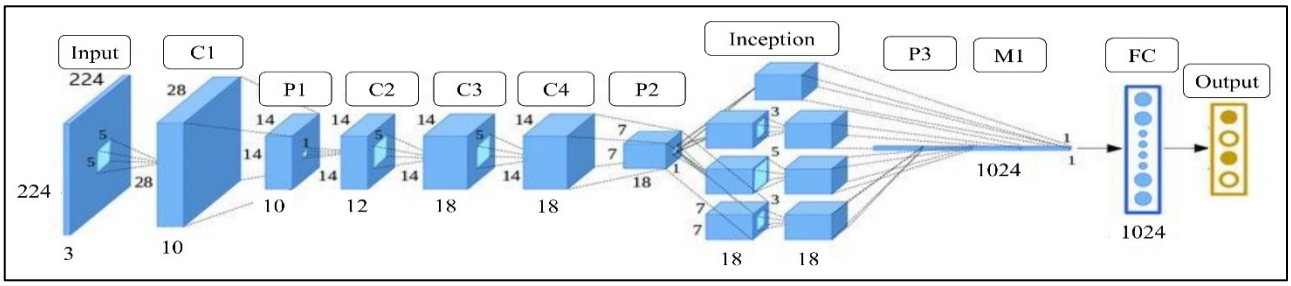

Figure 2. Simplified architecture of GoogleNet.

In order to extract features from images, these receptive fields generated operations in the new feature-map stack that captured sparse correlation patterns. In this study, we classified different kinds of brain tumours by extracting characteristics from MRI brain scans using the Google-Net model. Figure 3 shows the design of Google-Net. It uses three different-sized filters (1 × 1, 3 × 3, and 5 × 5) on the same image and merges their

features to get a strong result. The number of parameters is reduced from 138 million to 4 million by means of its 22 layers. Reducing dimensions is the purpose of introducing the (1 × 1) convolution. While training the network, this design identifies the optimal weight and characteristics [49,50]. Feature extraction by dimensionality reduction of convolution layers is illustrated in Figure 2.

3.3 DeepTumorNet

The DeepTumorNet model, which is a hybrid of CNNs, is based on their fundamental architecture. It could take months to train a convolution network from the beginning because it is a tough job. Hence, the suggested deep learning method would benefit from using an existing pretrained classifier for training rather than starting with a fresh deep learning classifier. Since GoogLeNet was still the victor in the ILSVRC (2014) ImageNet competition, we utilised it as a foundational model for this work. With 144 layers and 22 learnable ones, GoogLeNet includes 9 inception layer modules, 2 normalisation layers, 1 fully connected layer, 4 max pooling layers, 1 average pooling layer, and 2 convolution layers. One max-pooling layer and six convolutional layers made up each inception module. The GoogLeNet input layer was updated to 224 x 224 × 1. For the pretrained GoogLeNet method, the activation function ReLU was utilised. Simultaneously, the ReLU activation function treated zero as the only valid negative value. On the other hand, Leaky ReLU is an enhanced variant of ReLU that finds positive values to substitute for all negative ones. At the same time, the suggested DeepTumorNet classifier substitutes 15 more layers for the previous 5 in GoogLeNet. To further improve the expressiveness of the suggested model and get rid of the dying ReLU issue without messing with the main convolution neural network architecture, we switched the ReLU activation function in the feature map layer to the Leaky ReLU activation function. An increase of 144 to 154 layers was the result of these modifications. The architecture of the proposed DeepTumorNet approach is illustrated in Figure 3.

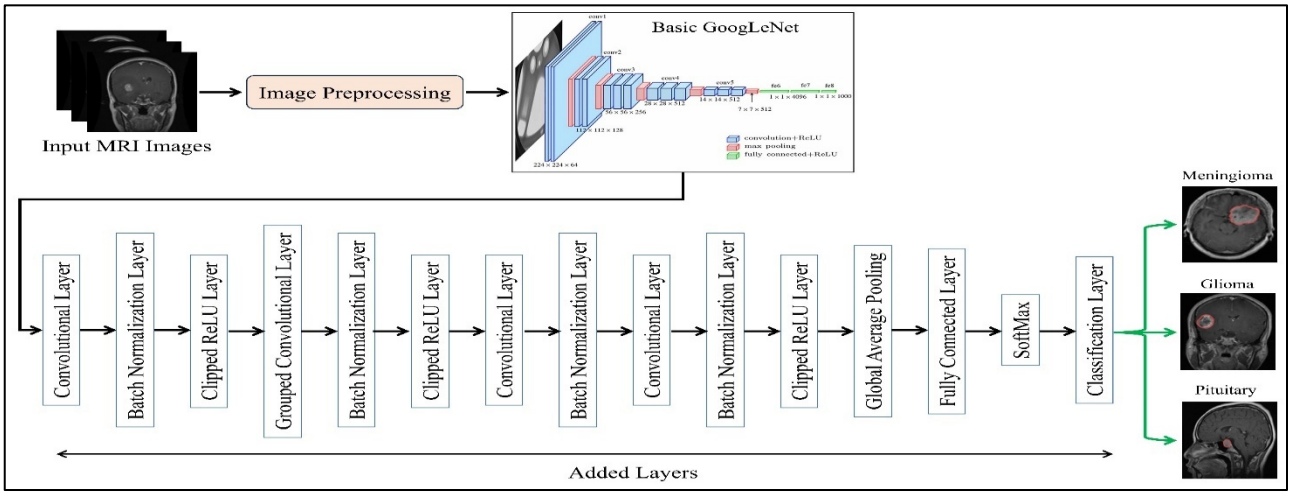

Figure 3. Architecture of the proposed model

The image size was instantly lowered by the first convolution layer's use of a 7 × 7 filter (patch) size. The 2 × 2 convolution block, which is the result of dimensionality reduction, was utilised by the second convolution layer, which had a depth of 2. Also, the inception module of Google ML offers various convolution kernels, such as 1 × 1, 3 × 3, and 5 × 5 convolution kernels, which extract features at different scales, beginning with the most delicate features and progressing to the core features. In order to calculate more features, a larger convolution kernel is better. In a similar vein, the 1 × 1 convolution kernel provides more information while decreasing the computational burden. The four convolutional layers that have been recently added have a very small filter size of 1 x 1. Moreover, we were able to achieve better features in terms of detail, accuracy, and robustness by increasing the CNN's number of convolution layers. In contrast to the first layer, which extracted low-level data, the four subsequent convolutional layers extracted high-level characteristics. The accuracy at the end of the network was also improved by the global average pooling layer. In addition, to address the dying ReLU issue and enhance the expressiveness of the proposed model, the feature map layer's ReLU activation function was replaced with the Leaky ReLU activation function. Classification performance was higher in the suggested hybrid model compared to the aforementioned state-of-the-art pretrained deep learning models since more detailed, discriminative, and deep features were extracted as a consequence of the extra layer. Table 3 provides more details about the additional layer, including its name, kind, number, size, and epsilon.

Table 3. Characteristics of added layers in the proposed hybrid model.

Layer Name	Type	No of Filter	Filter Size	Epsilon
Block 16 expand	Conv	950	1×1	
Block 16 expand BN	Batch Norm			0.01
Block 16 expand ReLU	Clipped ReLU Layer			
Block 16 depth-wise	Grouped Conv	950	3×3	
Block 16 depth-wise BN	Batch Norm			0.01
Block 16 depth-wise ReLU	Clipped ReLU Layer			0.01
Block 16 project	Conv	310	1×1	
Block 16 project BN	Batch Norm			0.01
Convolution 1	Conv	1270	1×1	
Convolution 1 BN	Batch Norm			0.01
Out ReLU	Clipped ReLU Layer			
Global average pooling 2d×1	Global Average Pooling			
Logits	Fully Connected			
Logits SoftMax	SoftMax			
Classification Layer Logits	Classification Layer			

3.3.1. Image Input Layer

In our example, the image input size was 224 × 224 × 1, and the suggested DeepTumorNet model began with the image layer, which included the model's input. For grayscale images, this is 1; for color images, it's 3, and it represents the width, height, and channel size of the input image. Before processing, the input layer reads the images [71-73].

3.3.2. Convolutional Layer

The convolutional layer was employed to create a feature map by recovering the deep learning features from an input image. In order to perform the mathematical process, two parameters are required: the image matrix and the size of the filters, which is defined as the height and width of the filters. In the convolutional layers of our hybrid model, we utilize various filter sizes of 7 × 7, 5 × 5, and 1 × 1, whereas in the max-pooling layers, we use 3 × 3. The "Padding" name-value combination is used by convolutional layers to add padding to the feature map input [69, 74]. One can get more details on the discrete-time convolution technique in Equation (1):

$$s(t) = (x * w)(t) = \sum_{a=-\infty}^{\infty} x(a)w(t-a) \quad (1)$$

where W stands for the kernel filter, x for the method's input, t for the time required, and s for the results. Equation (2) is taken into account when two-dimensional input data is being employed:

$$S(i,j) = (I * K)(i,j) = \sum_m \sum_n I(i,j) * K(i-m, j-n) \quad (2)$$

The areas of the desired matrix after the deep learning convolution approach are shown by terms i and j. The optimal method for this process is positioning the filter's centre at the top. To achieve cross-entropy using the proposed method, Equation (3) is applied:

$$S(i,j) = (I * K)(i,j) = \sum_m \sum_n I(i+m, j+n) * K(m,n) \quad (3)$$

3.3.3 Activation Function

Nonlinear transformation processes frequently make use of the activation functions in DL-based models. In the past, the most popular and extensively utilised activation functions that were developed were Sigmoid, Tanh, and ReLU. On the other hand, the dying ReLU problem occurs because ReLU outputs zero for all negative inputs, meaning that negative inputs are deactivated. The opposite side of a neuron is considered "dead" if it consistently produces no signal. To solve the dying ReLU problem, we substituted the feature map's ReLU with the leaky ReLU activation function, which is a value-added version of ReLU [6]. The negative number (x) output is actually a small linear component of x rather than zero when dealing with leaky ReLU. In addition, for the final fifteen layers, we employed a clipped ReLU activation function that carried out a

thresholding operation, setting any input value below zero to zero and any input value above zero to the given ceiling. Equations (4)–(8) represent the activation function formulas:

ReLU:

$$f(x) = \begin{cases} 0, x < 0 \\ x, x \geq 0 \end{cases}, f(x)' = \begin{cases} 0, x < 0 \\ 1, x \geq 0 \end{cases} \quad (4)$$

Sigmoid:

$$f(x) = \frac{1}{1+e^{-x}}, f'(x) = f(x)(1 - f(x)) \quad (5)$$

Tanh:

$$\tan\ h(x) = \frac{2}{1+e^{-2x}} - 1, f'(x) = 1f(x)^2 \quad (6)$$

Clipped ReLU:

$$f(x) = \begin{cases} 0, x < 0 \\ x0 \leq x < \text{ ceiling} \\ \text{ceiling}, x \geq \text{ ceiling} \end{cases} \quad (7)$$

Leaky ReLU:

$$f(x) = \begin{cases} x, x \geq 0 \\ \text{scale } * x, x < 0 \end{cases} \quad (8)$$

For positive inputs, the leaky ReLU function returns x; for negative inputs, it returns a tiny value, 0.01 times x. Therefore, in this scenario, no neuron is rendered inactive, and the presence of dead neurons is eliminated.

3.3.4 Batch Normalization Layer

In order to standardise the outputs produced by the suggested convolution layers, the batch normalisation layer was employed. As a result of normalisation, the suggested DeepTumorNet model can learn more efficiently and in less time during training. Equations (9 to 11) outline the steps for batch normalisation:

$$Yi = \frac{Xi - \mu\beta}{\sqrt{\sigma^2\beta + \varepsilon}} \quad (9)$$

$$\sigma\beta = \frac{I}{M}(Xi - \mu\beta)^2 \quad (10)$$

$$\mu\beta = \frac{1}{M}\sum_{i=1}^{M} Xi \quad (11)$$

Yi represents the new values gained from the normalisation operation, $\mu\beta$ stands for the stack's average value, $Xi = 1, \ldots, M, \mu\beta$ for the stack's standard deviation $\sigma\beta$.

3.3.5 Pooling Layer

A down-sampling technique was employed to reduce the size of the feature map and eliminate extraneous data after the convolution layer; this was followed by the pooling layer, which served to simplify the data obtained from the convolution layer. Most pooling algorithms use either average or maximal pooling. We employed global average pooling in the final fifteen layers. During pooling, the network refrains from learning anything. The pooling procedure made use of filters of a 3×3 size. Equation (12) lays out the steps for pooling:

$$S = w2 \times h2 \times d2 \quad (12)$$

$$w2 = \frac{(w1 - f)}{A+1} \quad (13)$$

$$h2 = \frac{(h1 - f)}{A+1} \quad (14)$$

$$d2 = d1 \quad (15)$$

in which $w1$ stands for the MRI images' width, $h1$ for the input images' height, $d1$ for the input images' depth, f for the filter size, A for the number of steps used, and S for the manufactured image's size.

3.3.6 Fully Connected Layer

A fully connected layer follows the convolutional layers in the suggested model. To do this, we combine the features learnt by the previous layers over several images. Images are sorted into categories by this layer, which finds the most important patterns. Since there are three classes in the planned study—meningioma, glioma, and pituitary—the output size value in the final fully linked layer is 3. A result of using the suggested FC layer for this purpose is 3. For this, we draw on Equations (16) and (17):

$$ui^I = \sum_j wjt^{l-1} yj^{l-1} \quad (16)$$

$$yi^I = f(ut^l) + b^{(l)} \quad (17)$$

This is where l represents the total number of layers, i and j represent the total number of neurons, and y/i represents the value created in the suggested output layer. $w_l - 1_{ji}$ represents the weight value of the hidden layer, $y_l - 1_i$ represents the value of the input neurones, u_{li} represents the value of the output layer, and $b(l)$ represents the value of deviation.

3.3.7 SoftMax Layer

The completely linked layer's output is made more normalised by the activation function. For each class, SoftMax generates positive values by executing the network's probabilistic calculation. In Equation (18), we can see the SoftMax algorithm stated:

$$P(y = j \mid xi, W, b) = \frac{\exp^{x^T W_j}}{\sum_{j=1}^{n} \exp^{x^I W_j}} \quad (18)$$

where the weight vectors are A, s, W, and b. Using each input, the classification layer—the last layer of the proposed model—generates the output. A probability distribution was returned by the SoftMax activation function [61].

RESULTS

The purpose of this research work was to accurately classify three different types of BT MRI images. A DeepTumorNet model and pre-trained deep learning models were employed to classify the CEMRI dataset; a portion of the dataset, 30%, was reserved for testing, while 70% was utilized for training. The findings were obtained using a machine with an i5 processor and 8 GB of RAM in a Python environment. To find out how well a deep learning network classifies data, one can use one of several methods. When running a CNN classification operation, a confusion matrix is frequently employed. Metrics like F1 score, recall, accuracy, and precision were highly sought after and favoured. A confusion matrix is used to make these calculations [62]. This study used standard evaluation measures, including recall, accuracy, and precision, to assess the proposed use of hybrid deep-learning classification based on CNN architecture for grading brain tumours as gliomas, meningiomas, and pituitary tumours. The suggested model's capabilities are measured by these attributes. Based on true positive (T.positive), true negative (T.negative), false positive (F.positive), and false negative (F.negative), the following are assessed. The following is a more in-depth explanation of metrics: A model's accuracy proportion of instances with a specific level of correctness relative to the total number of cases, is a measure of its correctness and quality. The following equation is used to calculate accuracy:

$$\text{Accuracy} = \frac{T.\text{negative} + T.\text{positive}}{T.\ \text{Negative} + F.\ \text{Positive} + F.\text{positive} + T.\text{positive}} \quad (19)$$

The accuracy of a model's classifications is defined by its precision. Here is the equation that is used to determine the equation of precision:

$$\text{Precision} = \frac{T \cdot positive}{T \cdot positive} + F \cdot \text{positive} \quad (20)$$

Specificity is used to estimate the model's efficiency. The following is the specificity equation:

$$\text{Specificity} = \frac{T.positive}{T.Positive + F.Positive} \quad (21)$$

The degree of accuracy in categorization is provided by the F-measure. The F-measure equation is provided below:

$$F - \text{measure} = 2 \times \frac{\text{precision} \times \text{Recall}}{\text{precision} + \text{Recall}} \quad (22)$$

An evaluation of a measure that shows competent classification is provided by the recall measure. The recall's equation is provided below:

$$\text{Recall} = \frac{T.\text{positive}}{T.\ \text{positive} + F.\ \text{negative}} \quad (23)$$

The suggested method's main contribution is the creation of a competitive and clinically applicable approach to the automated categorisation of brain tumours in various application contexts. In such cases, it may be necessary to use MRI images acquired using different imaging protocols and to distinguish between different kinds of brain tumours, even when additional intracranial tumours are present. Figure 4 shows the classification of brain tumours from MRI images using our suggested model's qualitative segmentation results.

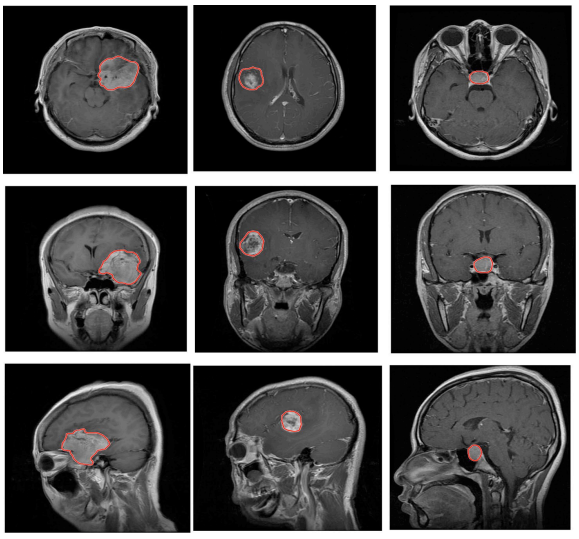

(a) (b) (c)

Figure 4. Classification of brain tumor, (a) Meningioma, (b) Glioma, and (c) Pituitary

In addition, the accuracy, precision, recall, and F1 score were tested after the proposed DeepTumorNet model was categorised, as shown in Figure 5. In terms of accuracy, precision, recall, and F1 score, the suggested DeepTumorNet model achieved 96.45%, 95.32%, 96.01%, and 95.20%, respectively.

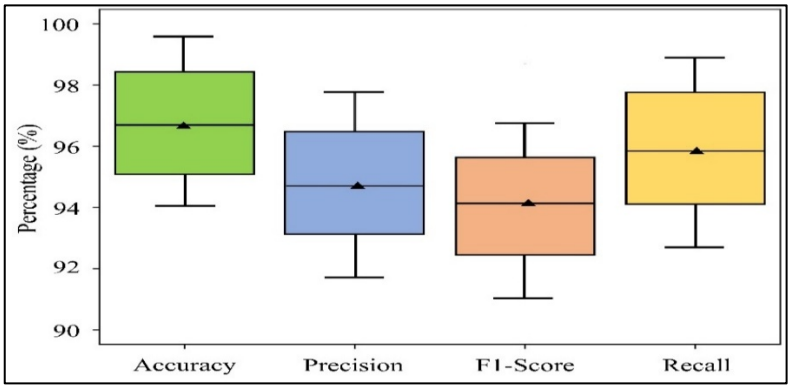

Figure 5. Quantitative evaluation of the proposed model

Figure 6 displays the accuracy and loss curves for the proposed DeepTumorNet method. The suggested model's performance in classifying images of tumours into fine-grained types (gliomas, meningiomas, and pituitary) is shown by the loss function. It was shown that the suggested hybrid method correctly detected brain tumours even at lower epochs than 80 [13] since the loss and accuracy of the model remained about the same after epoch 50. Figure 7 shows the train-and-validation confusion matrix of our proposed DeepTumorNet model, which summarizes the right and wrong classifications made by our technique.

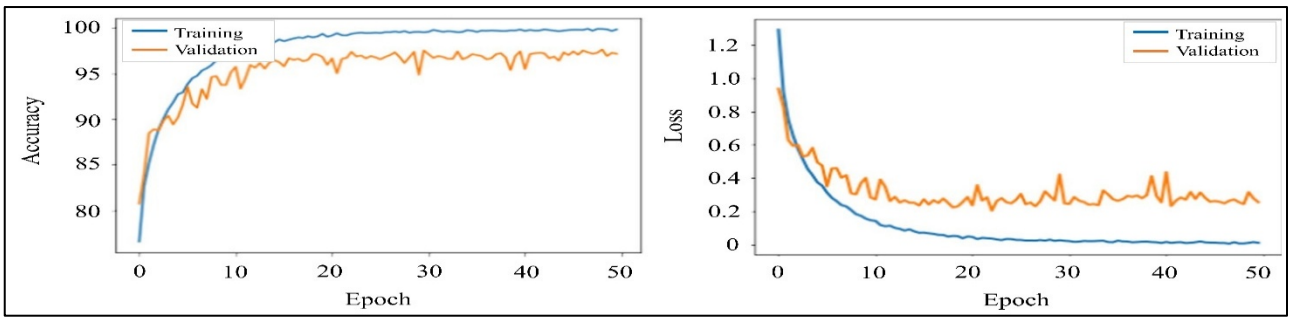

Figure 6. Training and validation analysis over 50 epochs

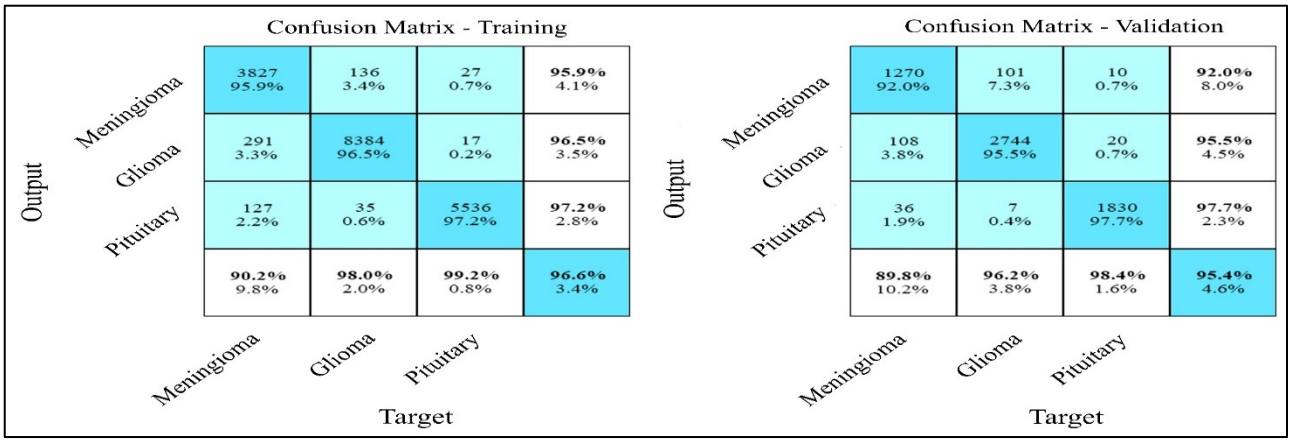

Figure 7. Confusion matrices for the original dataset with a record of the training and validation datasets.

Network output classes are represented by non-white rows in confusion matrices, while genuine classes are represented by non-white columns. The diagonal displays the numbers or percentages of correctly

classified images. Sensitivity is shown in the last row, and specificity in the last column. The bottom-right field displays the overall accuracy. Inside the non-white boxes, the top number indicates the total number of images, while the lower number indicates the training or test set proportion relative to the entire class database. Relevant studies on BTs utilising various DL approaches and a comparable dataset have been previously undertaken. Nevertheless, there were studies that relied on fewer images with many classes (fine-grained classification) rather than the more common binary classification (malignant vs. benign). When compared to the state-of-the-art methods in the literature, Table 4 clearly shows that the performance values of the suggested hybrid model, which is based on deep learning, were improved. We went over the results from the literature's state-of-the-art methods and compared them to our suggested DeepTumorNet method [17, 18, 19, 22, 24, 26].

Table 4. Experimentation results of pretrained models

Method/Teams	Accuracy (%)	Precision (%)	Recall (%)	F1-Score (%)
Liu et al. [1]	94.93	94.00	95.10	88.40
Ayaz et al. [3]	87.83	×	×	86.10
Rehman et al. [12]	94.61	×	90.20	91.10
Zhang et al. [9]	88.24	×	87.10	88.20
Masood et al. [13]	92.81	×	90.30	92.30
Hakim et al. [17]	94.30	92.10	×	89.10
Shanak et al. [11]	91.60	90.90	88.10	×
Zhu et al. [18]	93.10	92.30	92.20	×
Rani et al. [8]	92.20	92.70	91.80	89.70
This work	**96.45**	**95.32**	**96.10**	**95.20**

The results showed that DeepTumorNet was more effective than these other methods. The use of computationally more complicated hand-crafted engineering was also crucial for categorisation. With the addition of newly-created layers and the leaky ReLU activation function, the suggested model's 154-layer architecture mitigated the dying ReLU issue. As a result, the suggested hybrid model was able to identify more accurate features for classification and extract more descriptive and discriminative details. The suggested hybrid model is based on GoogLeNet, which has been enhanced by inserting 15 additional layers and swapping out the ReLU activation function for leaky ReLU. When compared to the base model GoogLeNet, the newly suggested technique achieved higher classification accuracy. Reduced hardware requirements characterise the DeepTumorNet model's convolutional neural network design. A period that works well for training is also necessary. The network's temporal complexity increased as the number of epochs and dataset sizes increased. On the other hand, the suggested hybrid model that relies on deep learning was able to extract deep features that were more descriptive, detailed, and discriminative. For BT categorisation in real-time, the suggested model can be integrated into an MRI machine. Neurologists and surgeons will also find it useful while treating BT patients [75].

CONCLUSION

Using a variety of convolutional neural networks and an innovative hybrid model, this study set out to categorize BTs. The proposed DeepTumorNet framework adopted the GoogLeNet architecture as its foundation. In order to improve GoogLeNet, 15 additional deep layers were added, replacing the previous 5 levels. In addition, the leaky ReLU activation function was used instead of the ReLU activation function, and the core convolution neural network architecture remained unaffected. Following the modifications, the overall number of layers rose from 144 to 154. The suggested hybrid model achieved record-breaking results in terms of classification accuracy (96.45%), precision (95.32%), recall (96.01%), and F1 score (95.20%). The experimental findings proved that the suggested hybrid model distinguished the brain tumors with greater precision. When compared to existing state-of-the-art methods, the suggested method outperformed them due to its accurate features for brain tumor classification and its increased computation of descriptive and discriminative data [76].

REFERENCES

1. Liu, X., & Liu, J. (2024). Aided Diagnosis Model Based on Deep Learning for Glioblastoma, Solitary Brain Metastases, and Primary Central Nervous System Lymphoma with Multi-Modal MRI. Biology, 13(2), 99.
2. Nahiduzzaman, M., Abdulrazak, L. F., Kibria, H. B., Khandakar, A., Ayari, M. A., Ahamed, M. F., ... & Kowalski, M. (2025). A hybrid explainable model based on advanced machine learning and deep learning models for classifying brain tumors using MRI images. Scientific Reports, 15(1), 1649.
3. Ayaz, H., Oladimeji, O., McLoughlin, I., Tormey, D., Booth, T. C., & Unnikrishnan, S. (2024). An explainable deep learning model for multi-modal MRI grading of IDH-mutant astrocytomas. Results in Engineering, 24, 103353.
4. Puranam Revanth Kumar, and Rajesh Kumar Jha "BrainHyperintensities: Automatic Segmentation of White Matter Hyperintensities in Clinical Brain MRI Images using Improved Deep Neural Network", The Journal of Supercomputing, pp. 1-37, 2024.
5. Mostafa, H., Haddad, N., Mohamed, H., & Taha, Z. A. E. H. (2024). Brain MRI Classification and Segmentation of Glioma, Pituitary, and Meningioma Tumors Using Deep Learning Approaches. In 2024 Intelligent Methods, Systems, and Applications (IMSA) (pp. 482-488). IEEE..
6. Yan, C., Liu, F., Peng, Y., Zhao, Y., He, J., & Wang, R. (2024). 3D convolutional network with edge detection for prostate gland and tumor segmentation on T2WI and ADC. Biomedical Signal Processing and Control, 90, 105883.
7. Celik, M., & Inik, O. (2024). Development of hybrid models based on deep learning and optimized machine learning algorithms for brain tumor multi-classification. Expert Systems with Applications, 238, 122159.
8. Rani, K.V., Sumathy, G., Shoba, L.K. et al. Gaussian weighting—based random walk segmentation and DCNN method for brain tumor detection and classification. Multimed Tools Appl (2024).
9. Zhang, W., Chen, S., Ma, Y., Liu, Y., & Cao, X. (2024). ETUNet: Exploring efficient transformer-enhanced UNet for 3D brain tumor segmentation. Computers in Biology and Medicine, 171, 108005.
10. Ye, Y., Zheng, X., Chen, T. et al. Computed tomography/magnetic resonance imaging for mandibular boundary invasion of oral squamous cell carcinoma assessment. BMC Oral Health 24, 172 (2024).
11. Shanaka Ramesh Gunasekara, H. N. T. K. Kaldera, Maheshi B. Dissanayake, "A Systematic Approach for MRI Brain Tumor Localization and Segmentation Using Deep Learning and Active Contouring", Journal of Healthcare Engineering, vol. 2021, Article ID 6695108, 13 pages, 2021.
12. Rehman, Z. U., Zia, M. S., Bojja, G. R., Yaqub, M., Jinchao, F., & Arshid, K. (2020). Texture-based localization of a brain tumor from MR images by using a machine learning approach. Medical Hypotheses, 141, 109705.
13. Masood M, Nazir T, Nawaz M, Mehmood A, Rashid J, Kwon H-Y, Mahmood T, Hussain A. A Novel Deep Learning Method for Recognition and Classification of Brain Tumors from MRI Images. Diagnostics. 2021; 11(5):744.
14. N. Arivazhagan, K. Somasundaram, D. Vijendra Babu, M. Gomathy Nayagam, R. M. Bommi, Gouse Baig Mohammad, Puranam Revanth Kumar, Yuvaraj Natarajan, V. J. Arulkarthick, V. K. Shanmuganathan, K. Srihari, M. Ragul Vignesh, Venkatesa Prabhu Sundramurthy, "Cloud-Internet of Health Things (IOHT) Task Scheduling Using Hybrid Moth Flame Optimization with Deep Neural Network Algorithm for E Healthcare Systems", Scientific Programming, vol. 2022, Article ID 4100352, 12 pages, 2022.
15. Chahal, P.K., Pandey, S. & Goel, S. A survey on brain tumor detection techniques for MR images. Multimed Tools Appl 79, 21771–21814 (2020).
16. Rao, C.S., Karunakara, K. Efficient Detection and Classification of Brain Tumor using Kernel-based SVM for MRI. Multimed Tools Appl 81, 7393–7417 (2022).
17. Hakim, A., Awale, R.N. Thermal Imaging - An Emerging Modality for Breast Cancer Detection: A Comprehensive Review. J Med Syst 44, 136 (2020).
18. Zhu, Z., He, X., Qi, G., Li, Y., Cong, B., & Liu, Y. (2023). Brain tumor segmentation based on the fusion of deep semantics and edge information in multimodal MRI. Information Fusion, 91, 376-387.
19. Puranam Revanth Kumar, B Shilpa, and Rajesh Kumar Jha "Brain disorders: Impact of mild SARS-CoV-2 may shrink several parts of the brain", Neuroscience & Biobehavioral Reviews, vol. 149, p.105150, 2023.
20. Hammouda, K., Khalifa, F., Soliman, A., Ghazal, M., El-Ghar, M. A., Badawy, M., Darwish, H.,

Khelifi, A., & El-Baz, A. (2021). A multiparametric MRI-based CAD system for accurate diagnosis of bladder cancer staging. Computerized Medical Imaging and Graphics, 90, 101911.

21. Tang, P., Zu, C., Hong, M., Yan, R., Peng, X., Xiao, J., Wu, X., Zhou, J., Zhou, L., & Wang, Y. (2021). DA-DSUnet: Dual Attention-based Dense SU-net for automatic head-and-neck tumor segmentation in MRI images. Neurocomputing, 435, 103-113.
22. Puranam Revanth Kumar, Rajesh Kumar Jha, and Amogh Katti "Brain Tissues Segmentation in Neurosurgery: A Systematic Analysis for Quantitative Tractography Approaches" Acta Neurologica Belgica, pp. 1-15, 2023.
23. Arabahmadi M, Farahbakhsh R, Rezazadeh J. Deep Learning for Smart Healthcare—A Survey on Brain Tumor Detection from Medical Imaging. Sensors. 2022; 22(5):1960.
24. Ranjbarzadeh, R., Bagherian Kasgari, A., Jafarzadeh Ghoushchi, S. et al. Brain tumor segmentation based on deep learning and an attention mechanism using MRI multi-modal brain images. Sci Rep 11, 10930 (2021).
25. Khan, S. R., Sikandar, M., Almogren, A., Ud Din, I., Guerrieri, A., & Fortino, G. (2020). IoMT-based computational approach for detecting brain tumors. Future Generation Computer Systems, 109, 360-367.
26. B Shilpa, Puranam Revanth Kumar, and Rajesh Kumar Jha, "LoRa DL: a deep learning model for enhancing the data transmission over LoRa using autoencoder", The Journal of Supercomputing, vol. 79, pp. 17079 –17097, 2023.
27. Rao, C.S., Karunakara, K. A comprehensive review on brain tumor segmentation and classification of MRI images. Multimed Tools Appl 80, 17611–17643 (2021).
28. Saleem, H., Shahid, A. R., & Raza, B. (2021). Visual interpretability in a 3D brain tumor segmentation network. Computers in Biology and Medicine, 133, 104410.
29. Gopi Kasinathan, Selvakumar Jayakumar, "Cloud-Based Lung Tumor Detection and Stage Classification Using Deep Learning Techniques", BioMed Research International, vol. 2022, Article ID 4185835, 17 pages, 2022.
30. Puranam Revanth Kumar, Amogh Katti, Sachi Nandan Mohanty, and Surender Nath Senapati, "A Deep Learning-based approach for an Automated Brain Tumor Segmentation in MR images", Pattern Recognition and Data Analysis with Applications, vol 888, pp. 87-97, 2022.
31. Díaz-Pernas, F. J., Martínez-Zarzuela, M., Antón-Rodríguez, M., & González-Ortega, D. (2021). A Deep Learning Approach for Brain Tumor Classification and Segmentation Using a Multiscale Convolutional Neural Network. *Healthcare (Basel, Switzerland)*, *9*(2), 153. https://doi.org/10.3390/healthcare9020153
32. Altwairgi, A. K., Raja, S., Manzoor, M., Aldandan, S., Alsaeed, E., Balbaid, A., Alhussain, H., Orz, Y., Lary, A., & Alsharm, A. A. (2017). Management and treatment recommendations for World Health Organization Grade III and IV gliomas. International journal of health sciences, 11(3), 54–62.
33. Ambuj Nandanwar. Aug 2023. The rise of FPGA technology in High-Performance Computing. https://www.design-reuse.com/article/61448-the-rise-of-fpga-technology-in-high-performance-computing/
34. Subrata et al., janv 2022. Texture, Morphology, and Statistical Analysis to Differentiate Primary Brain Tumors on Two-Dimensional Magnetic Resonance Imaging Scans Using Artificial Intelligence Techniques. https://doi.org/10.4258/hir.2022.28.1.46
35. Babu Vimala, B., Srinivasan, S., Mathivanan, S.K. et al. Detection and classification of brain tumors using hybrid deep learning models. Sci Rep 13, 23029 (2023). https://doi.org/10.1038/s41598-023-50505-6
36. T. Ruba et al., Accurate Classification and Detection of Brain Cancer Cells in MRI and CT Images using Nano Contrast Agents. https://dx.doi.org/10.13005/bpj/1991
37. Fatima et al., juil. 2023. Multi-class classification of brain tumor types from MR images using EfficientNets. 10.1016/j.bspc.2023.104777
38. Tsukamoto, T., & Miki, Y. (2023). Imaging of pituitary tumors: an update with the 5th WHO Classifications-part 1. Pituitary neuroendocrine tumor (PitNET)/pituitary adenoma. Japanese journal of radiology, 41(8), 789–806. https://doi.org/10.1007/s11604-023-01400-7
39. Pham, N. T., Rakkiyapan, R., Park, J., Malik, A., & Manavalan, B. (2023). H2Opred: a robust and efficient hybrid deep learning model for predicting 2'-O-methylation sites in human RNA. Briefings in bioinformatics, 25(1), bbad476. https://doi.org/10.1093/bib/bbad476

40. An et al., février 2019. Pharmacokinetic analysis for the differentiation of pituitary microadenoma subtypes through dynamic contrast-enhanced magnetic resonance imaging. https://doi.org/10.3892/ol.2019.10083.
41. Renlong Hang, et al. May 2020. Hyperspectral Image Classification with Attention Aided CNNs. https://deepai.org/publication/hyperspectral-image-classification-with-attention-aided-cnns
42. Youseef et al. Jan 2024. Dipper-throated optimization with deep convolutional neural network-based crop classification for remote sensing image analysis. https://peerj.com/articles/cs-1828/
43. Mark Ellison. Sept 2025. Old Tech Wins: SVM Outperforms AI in Music Genre Classification. https://www.kukarella.com/news/old-tech-wins-svm-outperforms-ai-in-music-genre-classification-p1756962000
44. Pankaj Singh. Feb 2024. A Must Read: 15 Essential AI Papers for GenAI Developers. https://www.analyticsvidhya.com/blog/2024/01/essential-ai-papers-every-gen-ai-developer-must-read/
45. Hussain, M., Thaher, T., Almourad, M. B., & Mafarja, M. (2024). Optimizing the VGG16 deep learning model with enhanced hunger games search for logo classification. Scientific reports, 14(1), 31759. https://doi.org/10.1038/s41598-024-82022-5
46. M. Ahmad, A. M. Khan, M. Mazzara, S. Distefano, M. Ali, and M. S. Sarfraz, "A Fast and Compact 3-D CNN for Hyperspectral Image Classification," in IEEE Geoscience and Remote Sensing Letters, vol. 19, pp. 1-5, 2022, Art no. 5502205, doi: 10.1109/LGRS.2020.3043710
47. Md Fahim Anjum. Aug 2024. Parkinson's Disease Classification via EEG: All You Need is a Single Convolutional Layer. https://arxiv.org/abs/2408.10457
48. Ahmed Bensaoud et al. Classifying Malware Images with Convolutional Neural Network Models. https://www.enhanceit.com/blog/classifying-malware-images-with-convolutional-neural-network-models
49. Boan, et al. A Mixed Reality Dataset for Deep Learning-Based Classification of MEP Systems. https://www.research.ed.ac.uk/en/publications/a-mixed-reality-dataset-for-deep-learning-based-classification-of/
50. Zhimeng Fan, et al. Feb 2021. Preparing State-of-the-Art Models for Classification and Object Detection with NVIDIA TAO Toolkit. https://developer.nvidia.com/blog/preparing-state-of-the-art-models-for-classification-and-object-detection-with-tao-toolkit/
51. Hitul Mistry. May 2025. How AI Agents Are Changing Medical Imaging and Radiology. https://digiqt.com/blog/ai-agents-in-medical-imaging-and-radiology/
52. Talaei Khoei, T., Ould Slimane, H. & Kaabouch, N. Deep learning: systematic review, models, challenges, and research directions. Neural Comput & Applic 35, 23103–23124 (2023). https://doi.org/10.1007/s00521-023-08957-4
53. Basil Kraft. Hybrid and explainable deep learning (HDL) Group. https://www.bgc-jena.mpg.de/en/bgi/hybriddeeplearning
54. Khan, H., Sajid, M. Z., Khan, N. A., Hamid, M. F., Youssef, A., Rehman, A., & Aburaed, N. (2025). An explainable deep learning-based feature fusion model for acute lymphoblastic leukemia diagnosis and severity assessment. *Frontiers in medicine*, *12*, 1694024. https://doi.org/10.3389/fmed.2025.1694024.
55. Caroline et al. Nov 2025. ------Comparison of CNN, VGG-19, and ResNet-50 Algorithm for Brain Tumor Detection. https://biomedpharmajournal.org/vol18octoberspledition/comparison-of-cnn-vgg-19-and-resnet-50-algorithm-for-brain-tumor-detection/
56. Lyu, Qing et al. “A transformer-based deep-learning approach for classifying brain metastases into primary organ sites using clinical whole-brain MRI images.” Patterns (New York, N.Y.) vol. 3,11 100613. 27 Oct. 2022, doi:10.1016/j.patter.2022.100613.
57. "From Traditional Methods to 3D U-Net: A Comprehensive Review of Brain Tumour Segmentation Techniques". written by Mushtaq Mahyoob Saleh, Musab Elkheir Salih, Mohamed A. A. Ahmed, Altahir Mohamed Hussein, published by Journal of Biomedical Science and Engineering, Vol. 18, No.1, 2025
58. Hossain. Mar 2026. Prediction of Cellular Malignancy Using Electrical Impedance Signatures and Supervised Machine Learning. https://arxiv.org/html/2601.04478v3
59. Sangdoo Yun et al. CutMix: Regularization Strategy to Train Strong Classifiers with Localizable Features. https://arxiv.org/pdf/1905.04899

60. Roman Panarin. Jan 2024. Basic Data Augmentation Method Applied to Time Series. https://maddevs.io/writeups/basic-data-augmentation-method-applied-to-time-series/

61. Santosh Gore. Apr 2023. Brain tumour segmentation and Analysis using the BraTS Dataset with the help of an improvised 2D and 3D UNet model. 10.21203/rs.3.rs-2791706/v1

62. Katoch, Sourabh et al. "A review on genetic algorithm: past, present, and future." Multimedia tools and applications vol. 80,5 (2021): 8091-8126. doi:10.1007/s11042-020-10139-6

63. Albalawi E, Thakur A, Dorai DR, Bhatia Khan S, Mahesh TR, Almusharraf A, Aurangzeb K, and Anwar MS (2024). Enhancing brain tumor classification in MRI scans with a multi-layer customized convolutional neural network approach. Front. Comput. Neurosci. 18:1418546. doi: 10.3389/fncom.2024.1418546

64. Yuki Wong et al. May 2025. Brain tumor classification using MRI images and deep learning techniques. https://journals.plos.org/plosone/article?id=10.1371/journal.pone.0322624

65. Kannan et al. Sept 2024. Brain Tumor Classification in MRI Using Hybrid ASA-Based Deep Learning and Masi-Entropy Multilayer Thresholding Segmentation with Sunflower Optimization. https://iieta.org/journals/ts/paper/10.18280/ts.420120

66. Gu, Yi, and Kang Li. "A Transfer Model Based on Supervised Multi-Layer Dictionary Learning for Brain Tumor MRI Image Recognition." Frontiers in neuroscience vol. 15 687496. 28 May. 2021, doi:10.3389/fnins.2021.687496

67. Abdusalomov, Akmalbek Bobomirzaevich et al. "Brain Tumor Detection Based on Deep Learning Approaches and Magnetic Resonance Imaging." *Cancers* vol. 15,16 4172. 18 Aug. 2023, doi:10.3390/cancers15164172

68. Jun Cheng, et al. Oct 2015. Enhanced Performance of Brain Tumor Classification via Tumor Region Augmentation and Partition. https://journals.plos.org/plosone/article?id=10.1371/journal.pone.0140381

69. Adrian Rosebrock. May 27, 2019. Keras: Feature extraction on large datasets with Deep Learning. https://pyimagesearch.com/2019/05/27/keras-feature-extraction-on-large-datasets-with-deep-learning/

70. Poola, Rahul Gowtham et al. "COVID-19 diagnosis: A comprehensive review of pre-trained deep learning models based on feature extraction algorithm." Results in engineering vol. 18 (2023): 101020. doi:10.1016/j.rineng.2023.101020

71. Rachel Draelos. Feb 2021. Designing Custom 2D and 3D CNNs in PyTorch: Tutorial with Code. https://glassboxmedicine.com/2021/02/06/designing-custom-2d-and-3d-cnns-in-pytorch-tutorial-with-code/

72. Madhav. Dec 2018. Getting started with Python OpenCV: Installation and Basic Image Processing. https://circuitdigest.com/tutorial/getting-started-with-opencv-image-processing

73. Adrian Rosebrock. Dec 2017. Image classification with Keras and deep learning. https://pyimagesearch.com/2017/12/11/image-classification-with-keras-and-deep-learning/

74. Koo, Peter K, and Sean R Eddy. "Representation learning of genomic sequence motifs with convolutional neural networks." PLoS computational biology vol. 15,12 e1007560. 19 Dec. 2019, doi:10.1371/journal.pcbi.1007560.

75. Nikolaj Buhl. July 2023. Activation Functions in Neural Networks: With 15 examples. https://encord.com/blog/activation-functions-neural-networks/

76. Semsary NA, Ahmed W, Amin K, Pławiak P, and Hammad M (2023). Improving sentiment classification using a RoBERTa-based hybrid model. Front. Hum. Neurosci. 17:1292010. doi: 10.3389/fnhum.2023.1292010